Four-color single molecule fluorescence with noncovalent dye labeling to monitor dynamic multimolecular complexes

Vanessa C. DeRocco[1,4], **Trevor Anderson**[2,4], **Jacob Piehler**[3], **Dorothy A. Erie**[1,*], and **Keith Weninger**[2,*]

[1] Department of Chemistry, The University of North Carolina at Chapel Hill, Chapel Hill NC 27599

[2] Department of Physics, North Carolina State University, Raleigh NC 27695

[3] Universität Osnabrück, Fachbereich Biologie, 49076 Osnabrück, Germany

Abstract

To allow studies of conformational changes within multi-molecular complexes, we present a simultaneous, 4-color single molecule fluorescence methodology implemented with total internal reflection illumination and camera based, wide-field detection. We further demonstrate labeling histidine-tagged proteins non-covalently with tris-Nitrilotriacetic acid (tris-NTA) conjugated dyes to achieve single molecule detection. We combine these methods to co-localize the mismatch repair protein MutSα on DNA while monitoring MutSα-induced DNA bending using Förster resonance energy transfer (FRET) and to monitor assembly of membrane-tethered SNARE protein complexes.

Keywords

FRET; MutS; Msh2; Msh6; DNA mismatch repair; SNARE proteins; Munc-18

Introduction

Single molecule fluorescence techniques including single-molecule Förster resonance energy transfer (smFRET) allow measurements of molecular associations and conformational changes during protein-protein and protein-nucleic acid interactions (1). Many important biological processes are amenable to single molecule studies by fluorescently labeling the molecules of interest and recording fluorescence emissions. Detection of three distinct single molecule fluorescence signals for multimeric colocalization or multiple FRET couplings have been demonstrated (2–9). Discrimination of single molecule fluorescence from 4 distinct dyes is used in a commercial DNA sequencing instrument employing zero mode waveguide sample chambers and prism-based spectral dispersion (10,11). This sophisticated instrument has not quantified FRET efficiency at single molecule level for 4 dyes. FRET interactions among 4 dyes on DNA have been recorded with a confocal microscope employing photodiodes for single point detection (12). Here, we present a simple modification of the typical two-color total internal reflection microscope (TIRM) that provides detection of single molecule fluorescence in 4 distinct

*To whom correspondence should be addressed: derie@unc.edu or keith_weninger@ncsu.edu, phone: (919) 962-6370 or (919) 513-3696.
[4]These authors contributed equally to this work

Competing interests
The authors declare no competing interests.

spectral channels simultaneously using wide-field imaging, and we demonstrate its capabilities for quantitative FRET studies (Fig. 1). Instrument construction is related to that used to characterize polarization and two-color FRET simultaneously (13). We combine this instrument with a tris-nitrilotriacetic acid (tris-NTA) dye-labeling to introduce a flexible approach for studying dynamics of multimeric complexes.

To dye-label proteins while preserving function, we use the recently developed tris-NTA-fluorophores(14,15). Ensemble FRET studies (16) used similar mono- and bis-NTA dyes, which bind 6-histidine tagged (6-his) proteins with micromolar affinities. In contrast, tris-NTA- fluorophores have subnanomolar to nanomolar binding constants for 6-his-proteins and dissociation rates on the order of 10^{-3} to 10^{-4} s^{-1}(15). The dye-bound state lifetimes of thousands of seconds are sufficient for most single molecule fluorescence experiments. A fluorescent dye is attached to the tris-NTA moiety via a 6-carbon linker (15) similar to the linker in commonly used covalently-linked dyes. This linker allows rotational flexibility for the dye, which is important for quantitative FRET applications. The non-covalent labeling is versatile, easily performed, and allows labeling proteins that do not tolerate more common labeling approaches. We demonstrate colocalization of a transient binding partner via its tris-NTA-fluorophore while simultaneously measuring conformational changes in the substrate using a FRET pair spectrally distinct from the tris-NTA dye with single molecule sensitivity for two different biological systems: one monitoring protein-induced DNA bending (yMutSα-mismatched DNA complexes) and the other monitoring protein-induced conformational changes in another protein (SNARE complexes). Both of these systems involve protein-induced conformational changes in the substrate that can be monitored by smFRET; however, independently colocalizing the binding partner confirms assembly of the complex.

Materials and Methods

Oligonucleotides

We purchased dye- and biotin-labeled oligonucleotides from Integrated DNA Technologies (Coralville, IA). The 50-bp Biotin/TAMRA-labeled oligonucleotide was 5′-Biotin-TGTCGGGGCTGGCTTAAGGTGTGAAATACCTCATCTCGAGCGTGCCGATA-TAMRA–3′. The Cy5-labeled 19-bp complement was 5′-TATCGGCACCCTCGAGATG-Cy5-3′ (underlined indicates CC base-base mispair). The unlabeled 31-bp complement was 5′-AGGTATTTCACACCTTAAGCCAGCCCC GACA–3′. The 50-bp and 19-bp oligonucleotides were annealed at ~65 °C for 20 min and slowly cooled to 55 °C. At 55 °C the 31 bp complement was added and the mixture was cooled to room temperature. (Figure 2A, B)

yMsh2-Msh6 protein

Expression and purification of 6-his tagged yMsh2-Msh6 (yMutSα) was performed as described (17). Dr. Thomas Kunkel (NIEHS, Research Triangle Park, NC) provided yMsh2 (pAC12 His-Msh2) and yMsh6 (yEpspGal Msh6) plasmids.

SNARE proteins

Expression and purification of full-length syntaxin-1A, soluble syntaxin-1A(1–263), SNAP-25, and soluble synaptobrevin(1–96) were as described (2,18,19). Unless indicated that 6-his tags were retained, 6-his tags were removed with thrombin as verified by SDS-PAGE. Munc-18 was expressed and purified as described(18) without 6-his tag removal.

SNARE proteins with combinations of indicated cysteine mutations introduced into cysteine free templates (syntaxin- e35c, s249c; synaptobrevin-s61c, a72c; SNAP-25-q20c-n139c) and

Munc-18 (containing all native cysteines) were labeled by mixing with 10-fold excess maleimide dyes (Alexa Fluors 488, 555 and 647; all Invitrogen, Carlsbad, CA) in 20 mM Phosphate, 200 mM NaCl, 100 μM TCEP, pH 7.4 overnight at 4C. Labeling efficiencies were 30% (syntaxin), 50% (synaptobrevin), >80% (SNAP-25) and 200% (Munc-18). Wild-type synaptobrevin(1–96) was labeled with Cy7-NHS (GE Healthcare, Piscataway, NJ) by incubating with equimolar dye in 20 mM Phosphate, 200 mM NaCl, pH 8, overnight at 4C, yielding 50% labeling. Synaptobrevin contains 2 central lysines (residues 52 and 59) and 5 C-terminal lysines (residues 83,85,87,91 and 94). Thus, we expect >70% of the Cy7-synaptobrevin to carry a C-terminally located dye. Note, optimization of labeling is important because the total four-color labeling efficiency of a multimeric complex is the product of individual efficiencies.

Parallel SNARE complex was formed from SNAP-25, His_6-synaptobrevin, and syntaxin as described elsewhere, including the 7M urea-buffer wash (19).

DNA Sample Preparation

Biotinylated dsDNA was incubated 10 min at 10 pM over biotinylated-BSA (Sigma-aldrich, St. Louis, MO)-streptavidin (Invitrogen) coated quartz slides as described elsewhere(20,21). All experiments were performed at room temperature in 20 mM Tris HCl, 100 mM sodium acetate, 5 mM magnesium chloride, 2% glucose, 0.1 mg mL^{-1} glucose oxidase, 0.025 mg mL^{-1} catalase, 2 mM 6-hydroxy-2,5,7,8-tetramethylchroman-2-carboxylic acid (Trolox) and 50 μM cyclooctotetraene all at pH 7.8 (all Sigma-Aldrich). No reducing agents were used to preserve the 6-His-Ni^{2+}-NTA complex.

SNARE Sample Preparation

Soluble SNARE complex was encapsulated at 33 nM per 3 mg ml^{-1} lipids in 100 nm egg phosphatidylcholine liposomes with 5% biotin-phosphatidylethanolamine lipids(22,23) (Avanti Polar Lipids, Alabaster, AL). The liposomes were formed with a syringe mini-extruder using 100 nm filters. The protein-containing liposomes were separated from free protein using gel filtration (SepharoseCL-4B) (GE Healthcare). Liposomes were tethered to biotinylated-BSA/streptavidin-coated quartz slides as described for the DNA samples. SNARE complex containing full-length syntaxin was reconstituted into supported bilayers as detailed elsewhere(18).

tris-NTA-Oregon Green Labeling

tris-NTA fluorescent dye conjugates were prepared as described elsewhere(14,15). We dye-labeled yMsh2-Msh6 by first incubating 10 nM tris-NTA-Oregon Green (NTA-OG) with 30 nM NiCl$_2$ for ~1 hr at room temperature. yMsh2-Msh6 (5 nM) was then incubated with 5 nM NTA-OG/15 nM NiCl$_2$(Ni$_3$NTA-OG) for ~1 hr on ice. Protein was not purified from unbound dye. 6His SNARE complexes were labeled with Tris-NTA-OG (Figure 3) as described in the results and discussion section below

Microscope

Fluorescence experiments were performed using a prism-type TIRM (Fig. 1) consisting of an IX51 microscope with a 60× 1.2 NA PlanApo water immersion objective (Olympus, Tokyo, Japan) and 4 collinear lasers for illumination (blue-473nm-50mW exciting OG or Alexa488; green-532nm – 50mW exciting TAMRA or Alexa555; red-635nm-40mW exciting Cy5 or Alexa647; infrared-690nm-50mW exciting Cy7). The lasers were individually shuttered to allow all combinations of simultaneous and sequential illumination. The microscope image was split into 4 distinct spectral bands by a Quadview imager (Photometrics, Tucson, AZ) and relayed onto quadrants of a Cascade 512B/emCCD

(Photometrics). The Quadview contained three dichroic mirrors (550dcxr, 645dcxr, 750dcxr, Chroma, Brattleboro, VT) and band pass filters to define the spectral bands: blue channel (513×17, Semrock, Rochester, NY), green channel (585×70, Chroma), red channel (685×70, Chroma), and infrared channel (794×160, Chroma). When the 690 nm laser was used a 640×100 nm filter (Chroma) was added to the red channel. Movies were collected at 10 Hz. A mapping function to align the 4 distinct spectral images was derived from images of TetraSpeck fluorescent microspheres (Invitrogen), which were visible in all channels. This mapping function was used to extract the other three dye emission intensities from locations pre-identified to contain the acceptor. Data was analyzed with custom MatLab routines (Mathworks, Inc. Natick, MA).

Backgrounds and leakages between channels were corrected during analysis as described elsewhere(3,5,6,8). Traces in figure 2C–E were corrected for background and leakage but not for gamma. We determined gamma factors from anti-correlated donor and acceptor photobleaching events using $\gamma = \Delta I_A / \Delta I_D$ (where $\Delta I_A = I_A^{\text{before bleach}} - I_A^{\text{after bleach}}$, and $\Delta I_D = I_D^{\text{after bleach}} - I_D^{\text{before bleach}}$) as described elsewhere(1,23,24). Gamma was determined from the data for figure 2F to be 2.16 for the Quadview. We confirmed that the same sample when measured with our 2-color single molecule FRET microscope yielded consistent FRET efficiency results (0.31) when using gamma specific for that instrument (0.94). Emission leakage between spectral channels was measured using single-labeled DNA samples. Transmission efficiencies of the blue, green, red, red with extra 640×100 filter, and infrared channels in our Quad-view system are 60%, 49%, 66%, 50%, and 65%, respectively of their value without the Quad-view dichroics and filters in place (bypass mode). Forty percent of Alexa488 signal level leaked into the green channel, 9% leaked into the red channel and none leaked into the infrared channel. No TAMRA signal was detected in the blue or infrared channels, 15% of the TAMRA signal leaked into the red channel. No Alexa555 emission was detected in the blue or infrared channels but 9% leaked into the red channel. There was no detectable emission from Alexa 647 in the blue, green, and infrared channels or from Cy7 in the blue, green, and red channels.

Observation protocols

Because blue dye photobleaching was limiting, we sometimes used a time-lapsed, shuttered blue illumination. This illumination scheme simplified interpretation of FRET between Alexa555 (or TAMRA) and Alexa647 because we could calculate FRET when the blue laser was not active. Undesired direct excitation of TAMRA and Alexa555 by blue light can complicate FRET measurements (3,5,6,8).

Figure 4 illustrates several excitation patterns. Sequential excitation is used first to excite Alexa647 (635 nm) followed by the excitation of Alexa488 (473 nm) to colocalize the acceptor and the auxiliary molecule (Figure 4B). Next, the donor Alexa555 is excited (532 nm) to observe FRET between the SNARE domains of Syntaxin 1A as reported by the high Alexa647 emission. In figure 4C, a laser sequence that allows for semi-continuous monitoring of Alexa488 labeled Munc-18 is used. The 635 nm laser is used to identify the acceptor Alexa647 dye and then is shuttered off at frame 5. The donor Alexa555 dye is excited (532 nm) at frame 10 and FRET to the acceptor is observed. The 473 nm laser is shuttered on for one frame at every 15th frame. The flashing laser pattern allows periodic monitoring of the Munc-18 colocalization while both prolonging the life of the blue dye and leaving frames for FRET calculation that are unaffected by the blue laser. The frames with 473 nm illumination are omitted from display in the red and green signals. Note the bleaching of Alexa488 after 8 seconds.

Results and discussion

The sequential and simultaneous FRET and colocalization experiments were performed with a prism-type TIRM, a Quadview splitter containing three dichroic mirrors, and an emCCD, allowing the simultaneous excitation and detection of the fluorescence from 4 dyes with emission spectra characteristic of Cy2, Cy3, Cy5 and Cy7 (Fig. 1 and methods). We first demonstrated this instrument by examining DNA bending induced by yMutSα. MutS homologs are responsible for recognizing and signaling repair of base-base mismatches and insertion-deletions in newly replicated DNA (25). MutS-mismatch complexes adopt multiple conformations with different degrees of DNA bending (from unbent to bend angles of ~ 90°) (20,26,27). It has been suggested that each bending state may have a different repair signaling potential (20,25,27).

Biotinylated DNA (50 base pairs) labeled with a FRET donor (TAMRA) and acceptor (Cy5) separated by 19 base pairs with a CC mismatch approximately halfway between the two fluorophores was tethered to a streptavidin-coated quartz surface (Fig. 2A, B). Because yMutSα contains over 30 cysteines, site-specific labeling using maleimide dye methodology is not feasible. Consequently, 6His-tagged-yMutSα (tagged on the N-terminal of Msh2) was non-covalently labeled using tris-NTA-OG (OG-yMutSα) (14). OG-yMutSα complexes were prepared before addition to CC-mismatch-DNA coated surfaces (methods). DNA bending was monitored by continuously exciting TAMRA with 532 nm illumination and measuring FRET to Cy5. The presence of OG-yMutSα was monitored by measuring OG emission under either continuous (data not shown) or pulsed (Fig. 2C–E) 473 nm illumination. Despite using an oxygen scavenging system, a shutter-pulsed scheme was required to allow longer observation intervals before OG photobleached.

After leakage subtraction and gamma correction (Methods), free CC-mismatch DNA molecules exhibit constant FRET efficiencies (Fig. 2C), with an average FRET ~ 0.35 (Fig. 2F). Unlabeled yMutSα binding increases FRET between TAMRA and Cy5, but yields no blue emission (Fig. 2D); whereas, binding of OG-yMutSα increases both FRET and the blue emission, consistent with the presence of the NTA-OG moiety (Fig. 2E). In addition, using a shuttered excitation (Fig. 2E), the presence of OG-yMutSα can be observed for long times indicating that the OG-NTA moiety remains stably bound to MutSα during the time course of the experiment. These long bound state lifetimes for tris-NTA dyes are consistent with ensemble experiments using NTA-dyes (14). In the absence of MutSα, the histogram of CC-DNA FRET efficiency *vs*. OG-yMutSα emission intensity for many molecules (Fig. 2F) shows FRET efficiencies around 0.35 and OG emission near zero. In the presence of OG-MutSα, one FRET emission peak overlaps with free DNA and another population shifted to higher FRET values (~0.6 gamma corrected) indicating yMutSα-induced DNA bending. A significant population of DNA without bound protein is expected because yMutSα is present at 5 nM, well below the 54 nM K_D (determined by fluorescence anisotropy). The higher FRET population can be divided into those with low or high OG emission. Those higher FRET events with low blue intensities suggest that unlabeled yMutSα is bound, and those with higher blue (15% of molecules) intensities confirm bound OG-yMutSα. To assess if tris-NTA-dye-labeling affects DNA bending, we compared DNA bending distributions for labeled and unlabeled MutSα and found no significant differences (Fig. 2F). These data demonstrate that fluorescently tagged yMutSα is active.

To demonstrate the method's flexibility, we examined interactions among neuronal SNARE proteins, which mediate membrane fusion (28). For neuronal SNAREs, two membrane proteins (syntaxin and synaptobrevin) on distinct cellular compartments assemble with a third SNARE protein (SNAP-25) to form a heteromeric complex of 4 parallel α-helices

called the SNARE complex, which crosslinks the fusing membranes through the transmembrane domains of the proteins (Fig. 3A).

Noncovalent labeling allows dyes to be added to samples in situ, as we demonstrated for membrane-incorporated SNARE complexes. 30 nM Ni_3-tris-NTA-OG was introduced above a phosphatidylcholine bilayer that contained SNARE complexes tethered by syntaxin's transmembrane domain (Fig. 3B). The complexes were tagged before assembly with Alexa647-maleimide covalently linked to S61C of synaptobrevin. We used simultaneous 473 nm and 635 nm illumination to identify individual Alexa647 labeled complexes by red emission while NTA-OG binding was assessed by blue emission (Fig. 3C). NTA-OG colocalized with over 25% of SNARE complexes when the 6His was present on synaptobrevin, and was reduced to background levels (1–4%) in controls (Fig. 3D).

Alternately, covalent labeling with 4 dyes can be used to structurally characterize this multiprotein complex. We prepared SNARE complexes with one donor-acceptor pair (Alexa 488/Alexa 555) at the N-terminal end of the α-helical bundle and a distinct donor-acceptor pair (Alexa 647/Cy7) at the C-terminal end. The SNARE complex is a 2 nm x 10 nm rod-like structure, so high FRET is expected from each pair, but little coupling is expected between the two pairs. Under continuous illumination with both blue and red lasers we simultaneously observed two independent FRET pairs on individual complexes (Fig. 4A).

The SNARE complex is also a binding platform for other proteins that regulate membrane fusion. We investigated Munc-18 binding to both syntaxin and to the SNARE complex (28,29). In the first SNARE experiment (Fig. 3A), syntaxin was covalently labeled with dyes at cysteine mutations in the C-terminal end of the SNARE domain and the N-terminal end of the 3-helix bundle that were designed to yield low (but non-zero) FRET (30) when the two domains connected by a flexible linker are unbound (open syntaxin) and high FRET when they bind (closed syntaxin). Syntaxin was reconstituted into supported lipid bilayers and Alexa488 labeled Munc-18 was added in solution above the bilayer. Using sequential red-blue-green laser illumination (top axis, Fig. 4B) we observed complexes where blue emission indicated the presence of Munc-18 and FRET in the green and red channels reported the conformational state of syntaxin. We confirmed that Munc18 binds to syntaxin in the closed conformation, as expected (30) (Fig. 4B).

We also observed Munc-18 interacting with the full SNARE complex (29). Soluble SNARE complex was co-encapsulated with Alexa488-Munc-18 in surface-tethered, 100 nm liposomes (Fig. 4C). The structure of this 4-protein complex is as yet undetermined. For this experiment, the SNARE complex was labeled with a donor dye (Alexa 555) in the 3-helix bundle of syntaxin and with an acceptor dye on synaptobrevin in the central region of the SNARE bundle. We screened liposomes for the presence of Alexa488-Munc-18 through blue dye emission under pulsed illumination and then used FRET in only those liposomes to examine the spacing between syntaxin's 3-helix bundle and the core SNARE complex (Fig. 4C). Measuring FRET from additional label attachment locations will allow us to put constraints on the overall conformation of the Munc18:SNARE complex.

Our development of a 4-color single molecule fluorescence instrument for measurements on immobilized biomolecules with wide-field imaging will allow single molecule studies of increasingly complex systems. The ability to colocalize binding partners at complexes while also monitoring conformational changes in other parts of the complex via FRET or to simultaneously monitor two FRET pairs on a single complex will enable studies of more complicated molecular assemblies than current approaches. This ability to directly correlate transient accessory binding to dynamic conformational transitions provides a new avenue for studies of biological signaling pathways. Simultaneous quantification of fluorescence

emission from 4 dyes interacting through FRET has the potential to report 6 distinct distances on a single molecular complex.

Furthermore, the demonstration that tris-NTA dye conjugates can label 6His-tagged proteins for single molecule studies significantly expands the capability for labeling proteins. Non-covalent labeling at a terminally located affinity tag can minimize the possibility of destroying function in proteins that are susceptible to structural perturbation by point mutations for dye attachment. The tris-NTA labeling approach also avoids the long incubation times required for most covalent labeling strategies and allows *in situ* labeling. The bound state lifetimes of the tris-NTA dyes to the 6His-tagged proteins are sufficiently long to permit monitoring of many protein-protein and protein-DNA interactions.

The ease of modifying an existing two-color TIRM by using a commercially available 4 color splitting device and its affordability as well as the flexibility of non-covalent dye labeling suggest this method could be adopted by many research groups.

Acknowledgments

References

1. Ha T, Ting AY, Liang J, Caldwell WB, Deniz AA, Chemla DS, Schultz PG, Weiss S. Single-molecule fluorescence spectroscopy of enzyme conformational dynamics and cleavage mechanism. Proc Natl Acad Sci U S A 1999;96:893–898. [PubMed: 9927664]

2. Bowen ME, Weninger K, Brunger AT, Chu S. Single molecule observation of liposome-bilayer fusion thermally induced by soluble N-ethyl maleimide sensitive-factor attachment protein receptors (SNAREs). Biophys J 2004;87:3569–3584. [PubMed: 15347585]

3. Clamme JP, Deniz AA. Three-color single-molecule fluorescence resonance energy transfer. Chemphyschem 2005;6:74–77. [PubMed: 15688649]

4. Friedman LJ, Chung J, Gelles J. Viewing dynamic assembly of molecular complexes by multi-wavelength single-molecule fluorescence. Biophys J 2006;91:1023–1031. [PubMed: 16698779]

5. Hohng S, Joo C, Ha T. Single-molecule three-color FRET. Biophys J 2004;87:1328–1337. [PubMed: 15298935]

6. Lee NK, Kapanidis AN, Koh HR, Korlann Y, Ho SO, Kim Y, Gassman N, Kim SK, Weiss S. Three-color alternating-laser excitation of single molecules: monitoring multiple interactions and distances. Biophys J 2007;92:303–312. [PubMed: 17040983]

7. Munro JB, Altman RB, Tung CS, Sanbonmatsu KY, Blanchard SC. A fast dynamic mode of the EF-G-bound ribosome. Embo J 2010;29:770–781. [PubMed: 20033061]

8. Ross J, Buschkamp P, Fetting D, Donnermeyer A, Roth CM, Tinnefeld P. Multicolor single-molecule spectroscopy with alternating laser excitation for the investigation of interactions and dynamics. J Phys Chem B 2007;111:321–326. [PubMed: 17214479]

9. Roy R, Kozlov AG, Lohman TM, Ha T. SSB protein diffusion on single-stranded DNA stimulates RecA filament formation. Nature 2009;461:1092–1097. [PubMed: 19820696]

10. Eid J, Fehr A, Gray J, Luong K, Lyle J, Otto G, Peluso P, Rank D, et al. Real-Time DNA Sequencing from Single Polymerase Molecules. Science 2009;323:133–138. [PubMed: 19023044]

11. Lundquist PM, Zhong CF, Zhao PQ, Tomaney AB, Peluso PS, Dixon J, Bettman B, Lacroix Y, et al. Parallel confocal detection of single molecules in real time. Opt Lett 2008;33:1026–1028. [PubMed: 18451975]

12. Heilemann M, Tinnefeld P, Sanchez Mosteiro G, Garcia Parajo M, Van Hulst NF, Sauer M. Multistep energy transfer in single molecular photonic wires. J Am Chem Soc 2004;126:6514–6515. [PubMed: 15161254]

13. Webb SE, Rolfe DJ, Needham SR, Roberts SK, Clarke DT, McLachlan CI, Hobson MP, Martin-Fernandez ML. Simultaneous widefield single molecule orientation and FRET microscopy in cells. Opt Express 2008;16:20258–20265. [PubMed: 19065164]

14. Lata S, Gavutis M, Tampe R, Piehler J. Specific and stable fluorescence labeling of histidine-tagged proteins for dissecting multi-protein complex formation. J Am Chem Soc 2006;128:2365–2372. [PubMed: 16478192]

15. Lata S, Reichel A, Brock R, Tampe R, Piehler J. High-affinity adaptors for switchable recognition of histidine-tagged proteins. J Am Chem Soc 2005;127:10205–10215. [PubMed: 16028931]

16. Kapanidis AN, Ebright YW, Ebright RH. Site-specific incorporation of fluorescent probes into protein: hexahistidine-tag-mediated fluorescent labeling with (Ni(2+):nitrilotriacetic Acid (n)-fluorochrome conjugates. J Am Chem Soc 2001;123:12123–12125. [PubMed: 11724636]

17. Clark AB, Cook ME, Tran HT, Gordenin DA, Resnick MA, Kunkel TA. Functional analysis of human MutSalpha and MutSbeta complexes in yeast. Nucleic Acids Res 1999;27:736–742. [PubMed: 9889267]

18. Weninger K, Bowen ME, Choi UB, Chu S, Brunger AT. Accessory proteins stabilize the acceptor complex for synaptobrevin, the 1:1 syntaxin/SNAP-25 complex. Structure 2008;16:308–320. [PubMed: 18275821]

19. Weninger K, Bowen ME, Chu S, Brunger AT. Single-molecule studies of SNARE complex assembly reveal parallel and antiparallel configurations. Proc Natl Acad Sci U S A 2003;100:14800–14805. [PubMed: 14657376]

20. Sass LE, Lanyi C, Weninger K, Erie DA. Single-molecule FRET TACKLE reveals highly dynamic mismatched DNA-MutS complexes. Biochemistry 2010;49:3174–3190. [PubMed: 20180598]

21. Li Y, Augustine GJ, Weninger K. Kinetics of complexin binding to the SNARE complex: correcting single molecule FRET measurements for hidden events. Biophys J 2007;93:2178–2187. [PubMed: 17513363]

22. Rhoades E, Gussakovsky E, Haran G. Watching proteins fold one molecule at a time. Proc Natl Acad Sci U S A 2003;100:3197–3202. [PubMed: 12612345]

23. Choi UB, Strop P, Vrljic M, Chu S, Brunger AT, Weninger KR. Single-molecule FRET-derived model of the synaptotagmin 1-SNARE fusion complex. Nat Struct Mol Biol 2010;17:318–324. [PubMed: 20173763]

24. McCann JJ, Choi UB, Zheng L, Weninger K, Bowen ME. Optimizing Methods to Recover Absolute FRET Efficiency from Immobilized Single Molecules. Biophys J 2010;99:961–970. [PubMed: 20682275]

25. Kunkel TA, Erie DA. DNA mismatch repair. Annu Rev Biochem 2005;74:681–710. [PubMed: 15952900]

26. Wang H, Yang Y, Schofield MJ, Du C, Fridman Y, Lee SD, Larson ED, Drummond JT, et al. DNA bending and unbending by MutS govern mismatch recognition and specificity. Proc Natl Acad Sci U S A 2003;100:14822–14827. [PubMed: 14634210]

27. Tessmer I, Yang Y, Zhai J, Du C, Hsieh P, Hingorani MM, Erie DA. Mechanism of MutS searching for DNA mismatches and signaling repair. J Biol Chem 2008;283:36646–36654. [PubMed: 18854319]

28. Rizo J, Rosenmund C. Synaptic vesicle fusion. Nat Struct Mol Biol 2008;15:665–674. [PubMed: 18618940]

29. Dulubova I, Khvotchev M, Liu S, Huryeva I, Sudhof TC, Rizo J. Munc18-1 binds directly to the neuronal SNARE complex. Proc Natl Acad Sci U S A 2007;104:2697–2702. [PubMed: 17301226]

30. Margittai M, Widengren J, Schweinberger E, Schroder GF, Felekyan S, Haustein E, Konig M, Fasshauer D, et al. Single-molecule fluorescence resonance energy transfer reveals a dynamic

equilibrium between closed and open conformations of syntaxin 1. Proc Natl Acad Sci U S A 2003;100:15516–15521. [PubMed: 14668446]
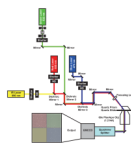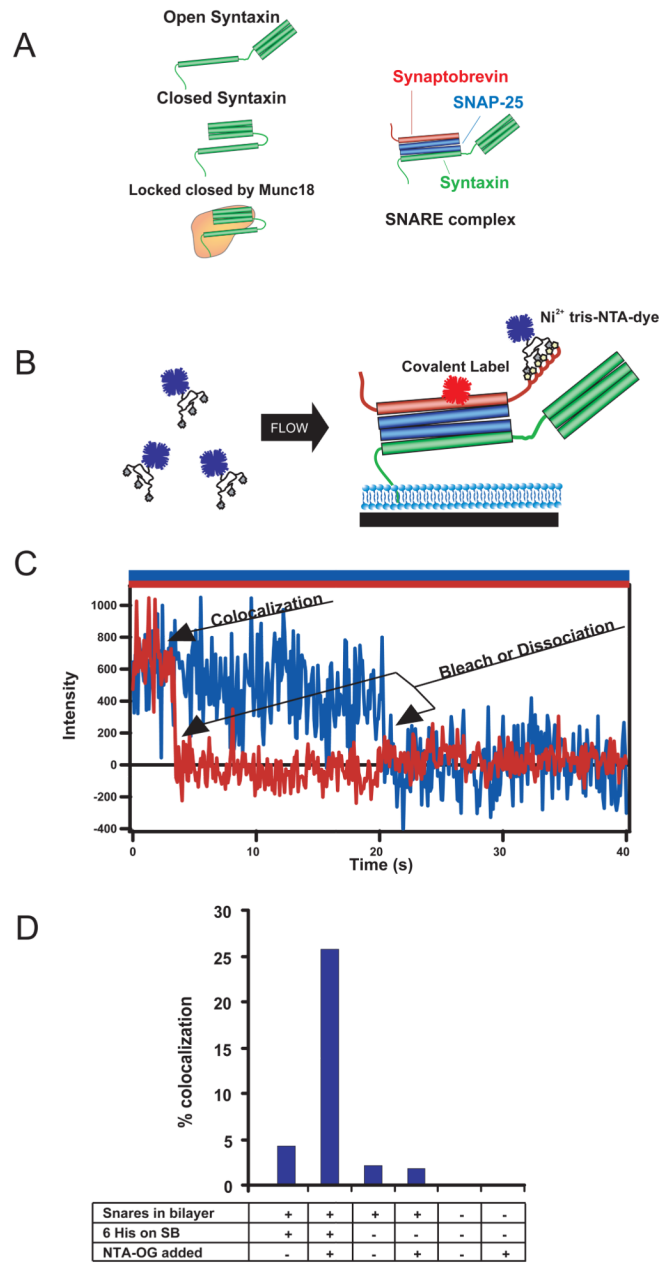
Figure 1.
Four-color single molecule TIRF microscope schematic. Simultaneous FRET and
colocalization experiments were performed using the prism-type total internal reflection
configuration. An Olympus IX51 inverted microscope with a 60× PlanApo water immersion
objective and a Quadview image splitter (550dcxr, 645dcxr, 750 dcxr) relayed the emitted
fluorescence to a Cascade 512B emCCD camera. Laser excitation was shutter controlled.
ND = neutral density filter; P= polarization dependent beamsplitter; λ/2 = half wave plate; λ/
4=quarterwave plate.
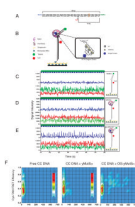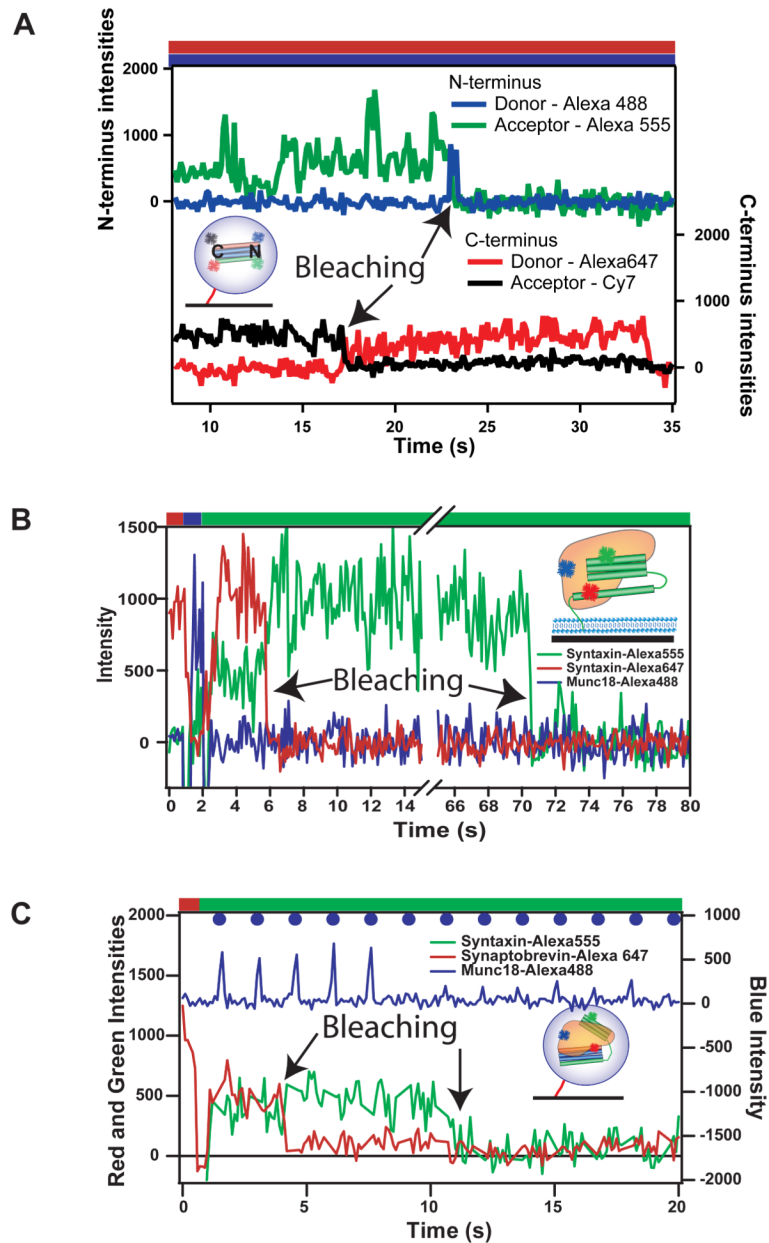
Figure 2.
yMutSα smFRET experiments. **(A**) DNA sequence of CC mismatch DNA containing a biotin tag, Cy5 label, and TAMRA label. **(B**) Cartoon describing the DNA functionalized quartz surface in the presence of tris-NTA Oregon Green labeled MutSα. **(C)** Emission from surface immobilized CC DNA labeled with Cy5 (red trace) and TAMRA (green trace). No colocalization is observed in the blue channel. **(D)** Emission from Cy5-TAMRA CC DNA exposed to unlabeled yMutSα. No colocalization is observed in the blue channel. **(E)** Emission from Cy5-TAMRA CC DNA bound by NTA-OG labeled yMutSα blue trace). **(F)** Three-dimensional histograms of Cy5-TAM FRET efficiency versus yMutSα-OG intensity in the presence and absence of 5 nM unlabeled yMutSα or tris-NTA-OG labeled yMutSα. The z-axis is the number of occurrences. Laser illumination pattern is indicated above each graph (blue=473nm, green=532nm, red=635nm).

Figure 3.
In situ labeling of SNARE proteins reconstituted in a supported lipid bilayer using tris-NTA dyes. **(A)** Schematic descriptions of syntaxin and the SNARE complex. **(B)** SNARE complex labeled by Alexa 647 at a cysteine mutation in synaptobrevin (s61c) is reconstituted into a 100% phosphatidylcholine supported lipid bilayer by the transmembrane domain of syntaxin. Tris-NTA-OG dye is added above the bilayer. **(C)** Simultaneous 473nm and 635nm illumination is used to colocalize the OG dye on synaptobrevin's 6-His tag with the covalently attached Alexa647. Synaptobrevin (1–96) is required to be incorporated in SNARE complex with SNAP-25 and syntaxin in order for it to localize to the bilayer. **(D)** Population analysis of colocalization (percentages) of Ni:NTA-OG from solution at sites preidentified to contain membrane incorporated SNARE complexes labeled with Alexa 647

(synaptobrevin a72c). Experiments using 6His-tagged synaptobrevin are compared to controls omitting the 6His-tag, Ni:NTA-OG, or SNARE complex as indicated.

Figure 4.
SNARE smFRET experiments. **(A)** SNARE complex lacking transmembrane domains was immobilized inside tethered liposomes and labeled with Alexa488 and Alexa555 on SNAP-25 (residues 20 and 139 – both near the SNARE complex N-terminus), Alexa 647 on syntaxin (residue 249 – near the SNARE complex C-terminus) and Cy7 on synaptobrevin (on a lysine, ~70% near the C-terminus). Two distinct FRET pairs on the same protein complex are simultaneously measured. **(B)** Emission from bilayer reconstituted, full-length syntaxin labeled with Alexa555 (green trace) and Alexa647 (red trace) (labels at residues 35 and 249) co-localized with Alexa488 labeled Munc-18 (blue trace). **(C)** Emission from liposome encapsulated SNARE complex lacking transmembrane domains labeled with Alexa555 (syntaxin-e35c) and Alexa647 (synaptobrevin-a72c) is co-localized with Alexa488 labeled Munc-18 (blue). Note, 473 nm laser is pulsed. In all panels, traces were

selected to show anticorrelated bleaching events to confirm single molecule FRET interactions. Laser illumination pattern is indicated above the graphs (blue=473nm, green=532nm, red=635nm, black=690nm).